RESEARCH ARTICLE

Innovation in potentiometry: 3D-printed polylactic acid-based ion-selective bulk electrode membranes

Ádám Golcs[1] · Brúnó Vermes[2,3] · David Christopher Siwek[1] · Péter Huszthy[1] · Tünde Tóth[1,4]

Abstract

Although ion-selective membrane-based potentiometric sensors have already proved their analytical performance in several fields of life, their applicability is still limited in practice. Biodegradable, ionic additive-free, polylactic acid-based bulk electrode membrane matrix containing various environmentally friendly polyethylene glycol derivatives as plasticizer was developed for the first time to replace the conventional PVC-based ones. Moreover, the first introduction of 3D printing in potentiometric chemosensing was also reported. It was demonstrated that a thoroughly optimized and generalizable procedure for filament extrusion combined with 3D printing technology provides a unique tool for series production of the redesigned ion-selective bulk electrochemical membranes. Finally, the potentiometric detection of Hg^{2+} in water was carried out as a proof-of-concept study on sensing. Results showed an unexpected improvement in electrochemical characteristics of the novel membranes compared to their conventional analogues. The present work expanded the practical applicability of conventional potentiometric cation-selective electrode membranes enabling their green, decentralized, and automated state-of-the-art manufacturing using a novel matrix composition.

✉ Ádám Golcs
golcs.adam@edu.bme.hu

1   Department of Organic Chemistry and Technology, Budapest University of Technology and Economics, Szent Gellért tér 4, 1111 Budapest, Hungary

2   Department of Polymer Engineering, Budapest University of Technology and Economics, Műegyetem rkp. 3, 1111 Budapest, Hungary

3   MTA-BME Research Group for Composite Science and Technology, Műegyetem rkp. 3, 1111 Budapest, Hungary

4   Institute for Energy Security and Environmental Safety, Centre for Energy Research, Konkoly- Thege Miklós út 29-33, 1121 Budapest, Hungary

Springer

Graphical abstract
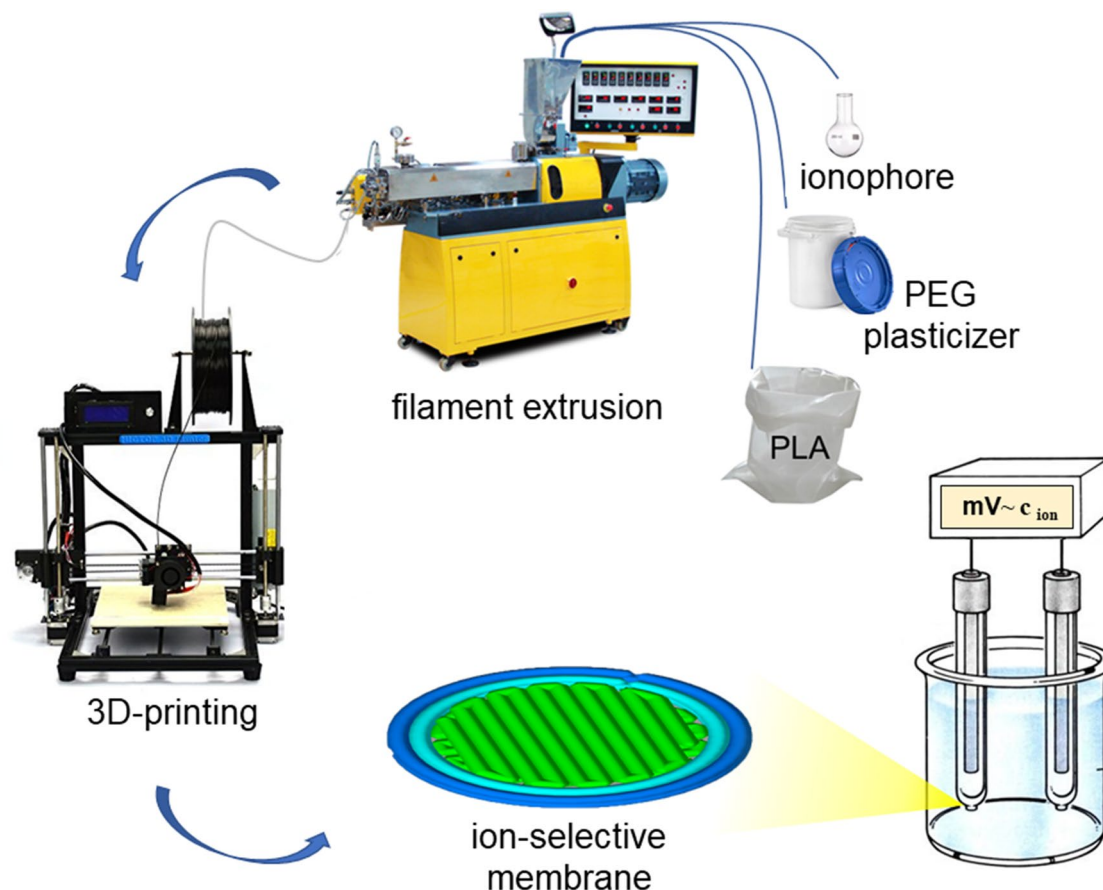
1 Introduction

Electrochemical ion-selective sensors have been widely used as *in situ* analyzers in medicine, environmental monitoring, and various areas of industry for many decades [1]. During this long period of time, countless efforts have been made to improve the operating parameters (i.e., limit of detection, selectivity), stability, portability, robustness, cost requirements, and environmental impact of these typically ion-selective membrane-based devices [2]. Over time, state-of-the-art technological advances, like electrohydrodynamic jet [3] or 3D printing [4–9] technology, have also emerged in the field of analytical chemistry. 3D printing offers tailored fabrication of geometrically diverse devices with practically unlimited designability, automation, and versatility of printable materials for any scientific problems. Examples include various applications in lab-on-a-chip advancement, additive manufacturing of sensing equipment, fabrication of microfluidic devices, selector membranes, nanoparticles, and electrodes as well [4–9].

Research on 3D printing of electrochemical sensing platforms is still in its early stage. The exponentially increased research interest of this field can be obviously seen from a search in the Web of Science® database entering 3D*, print*, and electrochem* as keywords. Although the first papers were published in the early 2010s, the total number of the reported works reached 1400 by January 2021 with more than 9300 citations during the previous year. Electrochemistry has been benefited from this technology mainly by customizing sensing approaches, especially electrode design [10–14]. Initially, the 3D-printed sensors used metals, which made them expensive and necessitated numbers of complicated post-treatments. Additionally, the limited range of their electrochemical potential also reduced the applicability [12, 15–17]. The appearance of carbon-based composite filaments helped to overcome these drawbacks allowing an unprecedently fast and cheap manufacturing of electrodes

[18, 19]. The thermoplastic matrix of printable materials is typically made of acrylonitrile butadiene styrene (ABS) or polylactic acid (PLA) and the sensors work based on amperometry or voltammetry [15]. In all cases, the principle of operation makes it essential for the applied materials to be conductive. Hence, these types of electrodes still show the disadvantages of strongly shape-dependent electrochemical behavior [20] and require additional post-treatment (e.g., chemical treatment with DMF, saponification with NaOH, or various electrochemical, biological or physical modifications) to provide electrically active surfaces by removing the charge transfer resistance polymer component from the surface of the composite electrode [15, 21]. Although much research today is focused on overcoming the disadvantages resulting from the intensively used concept of conductive material-based 3D-printed electrochemical sensors [18, 22–27], several conditions—i.e., graphene impurities and required surface modification—still remain unsolved [28, 29]. In summary, apart from the limitations of previously reported applications, 3D printing shows a great potential to open up novel perspectives in electrochemical sensing, such as in potentiometry.

Conventional, plasticized bulk ion-selective electrochemical membranes used for potentiometry are typically made of PVC, to which the plasticizer is added in an amount of approximately 2 mass equivalents related to the polymer [30]. They also contain lipophilic ionic sites in an amount of 1–2 wt%, which act as an ion exchanger to prevent ions with a charge opposite to the preferred analyte from entering the membrane and influencing the response signal. However, these ionic additives are mostly organic borate salts of weak stability and their leakage or decomposition is among the main causes of losing selectivity [30] and make conventional membranes of less advantages compared to covalently assembled sensor materials [31]. The ionophore is usually added to the other membrane components and then the mixture is dissolved in THF and poured into a mold in which the solvent evaporates to form a homogeneous polymer layer, from which the individual membranes are cut out and incorporated into an electrode body [32]. Therefore, it is not surprising that the major limitations of the widespread use of conventional potentiometric bulk membranes come from their cumbersome, small-scale, mechanical manufacturing technique. 3D printing provides a promising alternative to solve these problems.

Since the proposed 3D printing technology does not allow the application of the conventional PVC-based matrix of the ion-selective potentiometric membranes, a novel concept had to be applied. Among 3D-printable thermoplastic polymers, PLA is the most commonly used and commercially available one for creating structures of high diversity for industrial, medical, as well as for electrochemical applications. Moreover, it gains increasing popularity due

to its favorable properties (i.e., biocompatibility, modifiability) [21]. From an environmental point of view, PLA is also considered to be one of the most environmentally friendly polymers due to its biodegradability and sustainability [33, 34] and thus it was chosen as the matrix material for the proposed new type of membranes.

Herein, we report the development of a biodegradable PLA-based electrode membrane containing only environmentally friendly matrix components to replace the generally applied plasticized PVC backbone and to provide a greener alternative to conventional sensing membranes. Moreover, the reported electrochemical membranes do not contain any ionic additives. This simplified membrane composition can prevent the leakage of the charged agents into the mainly investigated aqueous samples. This reduced composition is applicable as PLA exhibits a weak negative charge on the polymer surface due to lactic acid contaminants resulting from its inevitable partial degradation [35]. According to the present studies this anionic content is able to act as an effective, immobilized ion-exchanger responsible for the permselectivity of the membranes toward cations. Subsequently, the experimental production of the novel-type ion-selective membranes was also performed, including the extrusion of the neutral ionophore-containing filament as well as the 3D printing of the electrode membranes with a detailed optimization of process parameters. Furthermore, as a proof of concept, the potentiometric determination of Hg^{2+} in water was also carried out. These studies showed unexpected advantageous properties over the application of conventional PVC-based bulk ion-selective electrode membranes. We hope that the present study will be a milestone in the practical application of cation-selective potentiometric analyzers possessing the ability of decentralized fabrication and providing a generally usable method for series production of bulk electrochemical membranes.

2 Experimental

2.1 Chemicals and apparatus

Starting materials were purchased from Sigma-Aldrich Corporation (St. Louis, MS, USA, owned by Merck) and used without further purification, unless otherwise noted. Ingeo™ Biopolymer 3100HP-type polylactic acid pellets (Nature-Works LLC, Minnetonka, MN, USA) were plasticized by polyethylene glycol derivatives with different average molecular masses, like PEG-400, PEG-1500, or PEG-monolaurate (M-PEG, Mn = 400) and used for extrusion. Solvents were dried and purified according to well-established methods [36]. A lipophilic acridono-18-crown-6 ether (Fig. 1) was synthesized [37], embedded in bulk polymer membranes, and used as a neutral ionophore.
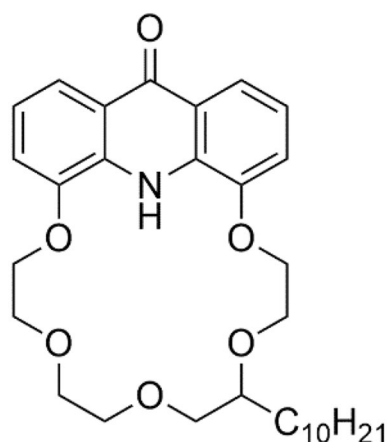
Fig. 1 Lipophilic acridono-crown ether neutral ionophore

For potentiometric measurements, a Philips IS-561 (Glasblaserei Moller, Zurich, Switzerland) electrode body was used with an Ag/AgCl/3 mol L^{-1} KCl//1 mol L^{-1} KCl double-junction reference electrode (Metrohm, Herisau, Switzerland) in a Radelkis OP-208/1 precision pH meter (Radelkis Ltd., Budapest, Hungary) in all cases. 10^{-3} mol L^{-1} mercury(II) acetate was used as the inner filling solution during calibration, while in the case of selectivity measurements, strongly discriminated 10^{-3} mol L^{-1} lithium(I) acetate was applied. Furthermore, membranes that had not been in contact with primary ions before were used for estimating selectivity constants to reduce the possibility of bias [38]. For pH measurements, a Mettler Toledo SevenEasy pH meter (Mettler Toledo, Columbus, Ohio, USA) fitted with a Mettler Toledo Inlab micro electrode was used. The various pH values were adjusted with concentrated nitric acid. The accuracy of pH determinations was within ± 0.1 unit. Each weight was determined by a Mettler Toledo XS105 microanalytical balance (Mettler Toledo, Columbus, OH, USA) to the nearest 0.1 mg. The pictures of the membranes were made using a Nikon SE-type clinical and laboratory optical microscope (Nikon Instruments Inc., New York, USA). A Jeol JSM 6380LA scanning electron microscope (SEM) was used in secondary electron imaging mode (SEI) for examining the membrane structure (Jeol Ltd., Tokyo, Japan) after a surface modification of the cross-sectional samples with a Jeol 1200 sputter coater (Jeol Ltd., Tokyo, Japan) using high-quality gold in argon plasma. The operating parameters were the following: accelerating voltage 10 kV, working distance 12 mm, and spot size 40 nm.

2.2 Filament extrusion and 3D printing of the ion-selective membranes

Extrusion of plasticized 3D printing-compatible polymer filament containing the ionophore was carried out using a Labtech LTE 26–44 twin-screw extruder (Labtech Engineering Co., Ltd., Samutprakarn, Thailand) with a screw diameter of 26 mm, volumetric dosing system, shared barrel and screws co-rotating and PLC control with a touch screen. Unplasticized pellets were dried at 80 °C for 24 h in a drying oven (Despatch LBB2-27-1CE, Despatch Industries, Glenview, IL, USA) as a pre-treatment and plasticized with the corresponding PEG derivative via the extrusion process.

The previously extruded filament was used for 3D printing of the membranes. Membrane design was first planned using CATIA 3D modeling software (Dassault Systèmes, Vélizy-Villacoublay, France). Fused deposition modeling was employed to fabricate the potentiometrically active structures with the diversely plasticized filaments containing the neutral ionophore. The 3D printing was performed with a Creality CR-10 S (Creality, Shenzhen, China) 3D printer controlled by PrusaSlicer software (Prusa Research, Prague, Czech Republic). A removable spring steel PEI 310×310-mm (suitable for printing about 300 membranes) print bed (ENERGETIC 3D Store, Shenzhen, China) was used as a build plate. Optimization of the main printing parameters—i.e., printing temperature of the individual layers, printing speed, the feed rate of the filament, and temperature of the print bed—had to be carried out for stable operation. The effects of these critical factors are discussed in Sect. 3. The membranes required neither post-treatment nor any kind of electrochemical activation before use.

2.3 Electrochemical measurements and evaluation of the results

All of the potentiometric measurements were carried out at ambient temperature (25 ± 1 °C). Illustration [39] of the potentiometric cell used for the present electrochemical studies is shown in Fig. 2. The ion-selective membrane was mechanically fixed in the plastic socket of the electrode body.

The electromotive force (EMF) of the cell was measured by varying the concentration of the stirred test solutions in the range from 10^{-9} to 10^{-1} mol L^{-1} by serial dilution with double-distilled water. During calibration, the EMF values were recorded both with increasing and decreasing concentrations. Each point of the diagrams is from four independent measurements. The deviation (measuring the same sample at least four times) was below ± 0.5 mV and the reproducibility (measuring four different samples of the same concentration after regeneration) was below ± 2.0 mV in every case, except for the measurements which were out of the working pH range. Between two different sample solutions, the electrode pair was washed with distilled water and then wiped off. The response time of the membrane sensors—i.e., the time in which stable and constant potentials were recorded—was determined by measuring the potentials at
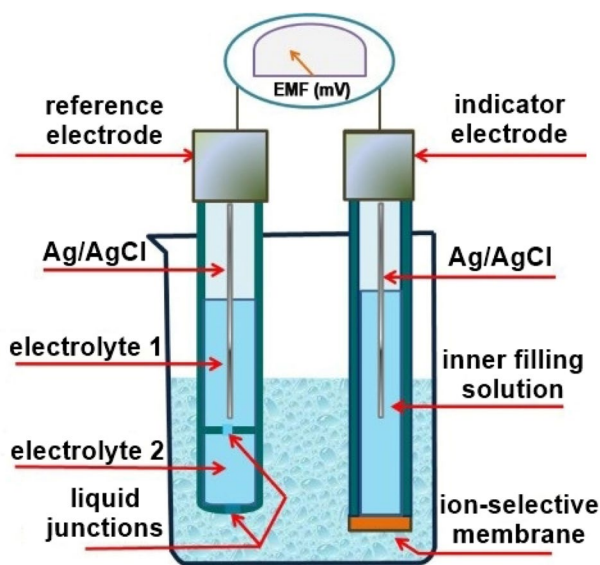
Fig. 2 Schematic representation of the applied potentiometric device

different times. The potential values were recorded in correspondence with the determined response time after immersing the electrode into a stirred test solution of 50 mL. Potentiometric selectivity coefficients ($\log K_{i,j}^{pot}$) are estimated by the separate solution method based on the *Nikolsky–Eisenman* equation from the EMF data measured for metal (Li$^+$, Na$^+$, K$^+$, Ag$^+$, Mg^{2+}, Cd^{2+}, Zn^{2+}, Co^{2+}, Ca^{2+}, Cu^{2+}, Pb^{2+}, Hg^{2+}) acetates according to Eq. 1:

$$\log K_{i,j}^{pot} = \frac{EMF_j - EMF_i}{S_i} + \log \frac{a_i}{a_j^{z_i/z_j}}, \quad (1)$$

where a_i and a_j are the ion activities of the preferred and the competing ion, respectively, which induce EMF_i and EMF_j potentiometric responses, S_i is the slope of the calibration curve as a function of a_i determined on its linear working range, while z_i and z_j represent the charges of the corresponding ions. Activity coefficients were calculated using the *Debye–Hückel* equation. The lower detection limit (LOD) was determined according to the standard definition based on a linear fitting on the near linear range of the calibration curve [30]. OriginPro 8.6 (OriginLab Corporation, Northampton, Massachusetts, USA) software was used to evaluate the results.

3 Results and discussion

3.1 Experimental production of novel ion-selective membranes

For 3D printing-based fabrication of electrochemical membranes, a 3D printer-compatible thermoplastic polymer-based filament containing the ionophore needs first to be prepared. It is a basic requirement for the matrix material of the membrane to be in plastic state to ensure sufficient permeability of the components of the sample solution [30]. Hence, the glass transition temperature (T_g) has to be around the application temperature (usually room temperature) or optimally below that. As PLA is a sustainable and biodegradable polymer and one of the most commonly used materials for 3D printing, it was chosen as membrane matrix. Due to the permeability requirements, plasticizers also had to be added. As environmentally friendly considerations were also an important aspect of the development, biocompatible PEG derivatives, specifically PEGs with different average molecular masses of 400 or 1500 g mol^{-1} or their monolaurate ester, were used as plasticizers in an amount of 10 or 20 wt% related to the PLA. Moreover, the addition of even a 10 wt% of the proposed PEG derivatives reduces the T_g of the PLA to less than 40 °C [40] and also provides a proper permeability for the most frequently investigated aqueous samples. (The use of additional ionic membrane components proved to be unnecessary due to the carboxylate content of the PLA, which provides a negative charge for the membrane [35].) In summary, the membranes were made of 99.7 wt% green materials, the remaining 0.3 wt% is the ionophore. The properties of the ionophores may differ individually; however, it is important to note that the applied technology requires the thermal stability of the ionophore (up to 190 °C) and its adequate lipophilicity for effective physical immobilization. Our experience shows (data not reported) that the use of less than 0.3 wt% ionophore results in a significant inhomogeneity of the membranes and a decrease in sensitivity during detection. On the other hand, the increasing amount of the ionophore does not significantly improve the operating parameters, thus 0.3 wt% ionophore was uniformly applied in the membranes. The instrumentation for filament extrusion is schematically illustrated in Fig. 3.

In the case of the applied equipment, the melted material flows from the extruder (A in Fig. 3) onto an air-cooled conveyor belt (B in Fig. 3) with a length of 2.5 m. Optionally, a vacuum calibration water bath can also be applied to gain high-precision filament line. Similarly, a haul off unit is also advisable for advanced production, but these additional devices were not used during the experimental
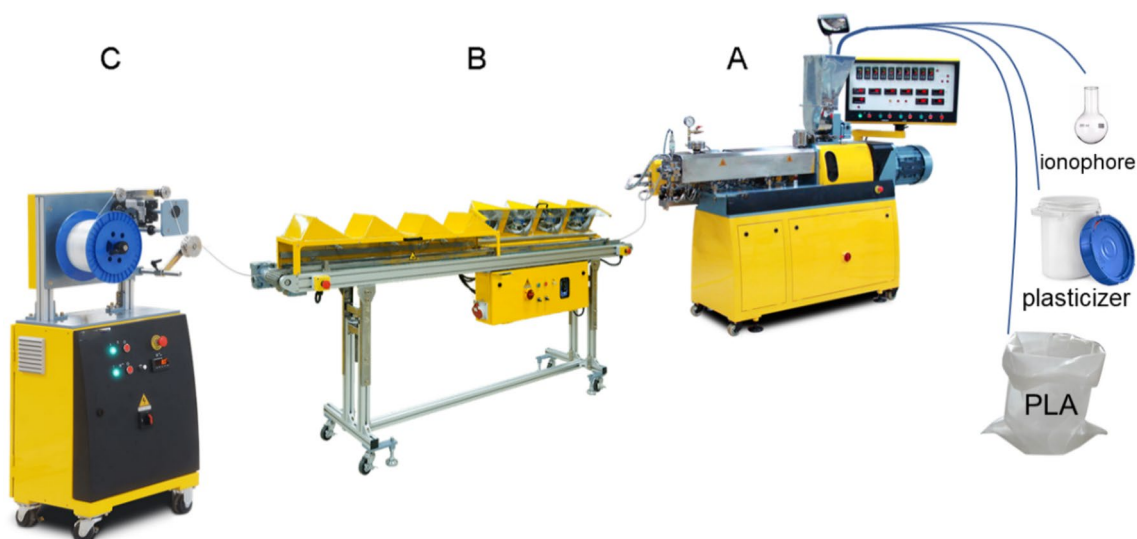
Fig. 3 Instrumentation for filament production

production. After passing through several filament guides, the polymer line is transferred to the wind-up station (C in Fig. 3). Until use, it is advisable to store the filament under airtight conditions due to its humidity-absorbent capability.

Each production batch started from 0.4 kg as a total amount of raw materials. Initially, the ionophore should be added homogeneously to the PLA granules used for filament extrusion. Since the ionophores make up only a small proportion of the membrane components, it is advisable to distribute them with the granules in the form of a solution. A 0.1 mol L^{-1} solution of the ionophore in ethyl acetate was added to the PLA granules (20 mL/batch). Ethyl acetate dissolves PLA well and thus it fixes the ionophore in the matrix material by etching the surface of the granules. After the granules are uniformly wetted, the solvent was evaporated at room temperature (4 h) to obtain the polymer granules containing the ionophores. As PLA is able to bind a large amount of water during storage, which significantly affects its processability, the granules were placed in a drying oven at 80 °C for 24 h. After removing the moisture, the plasticizer was added to the granules and the mixture was poured into the hopper of the preheated extruder. The initiation state is indicated by an increase in pressure, while the end phase of the process is indicated by a decrease in it. In the intermediate state, precise optimization of the raw material feed rate (controlled by the rotation speed of a screw in the throat), the extrusion rate (controlled by the rotation speed of the twin screw in the thermostated barrel) in connection with the fiber removal speed (controlled by the speed of the conveyor belt), and the temperatures of the extrusion zones in connection with the pressure are required to achieve suitable filament for 3D printing. The main operating parameters
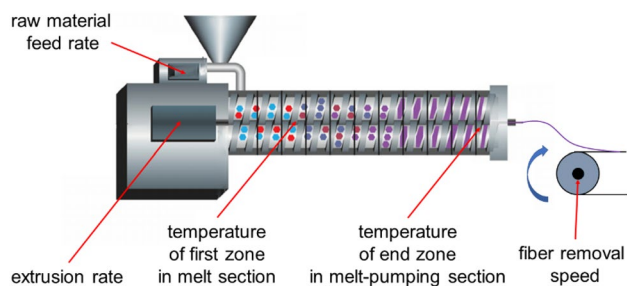

Fig. 4 Main process parameters influencing the filament production

of the extrusion process, which had to be optimized, are illustrated in Fig. 4.

The greatest challenge during extrusion is caused by the drastically changed rheological properties of PLA due to the plasticizer content, especially the extremely reduced viscosity of the melted polymer. This also strongly limited the plasticization of the polymer and thus it was not possible to produce a filament with a plasticizer content above 20 wt%. The process proved to be extremely sensitive to all of the five main operating parameters, which were examined (shown in Fig. 4). Fiber was only obtained when setting the optimized parameters. Even a 2% deviation from each optimized parameter value made fiber formation impossible. The values obtained as a result of the parameter optimization are shown in Table 1.

Although the optimal parameter values may slightly vary from device to device, data reported here can be useful starting points for any production. Under optimized conditions, fibers of 1.6 ± 0.5 mm diameter were successfully produced with all fiber compositions. A shaping die of 1.75 mm diameter was used and thus the diameter reduction was caused

Table 1 Optimized operating parameters for the filament extrusion process as a function of the applied plasticization

Membranes with different plasticizer [a]	Material feed rate (rpm)	Extrusion rate (rpm)	Temperature of first zone (°C)[b]	Temperature of end zone (°C)[b]	Fiber removal speed (m s^{-1})
10% PEG-400	4	10	160	180	0.22
20% PEG-400	5	12	160	180	0.31
10% PEG-1500	4	9	155	175	0.03
20% PEG-1500	4	15	155	175	0.04
10% M-PEG	3	8	165	185	0.20
20% M-PEG	10	15	165	185	0.38

[a]The amount of plasticizer required to achieve a near-*Nernstian* electrode response of the membranes was at least 10 wt%, while the upper technological limit of production was found to be 20 wt% plasticizer content for all PEG derivatives

[b]Between the temperatures of the two endpoints, the temperature of the heated extruder barrel changed gradually and proportionally
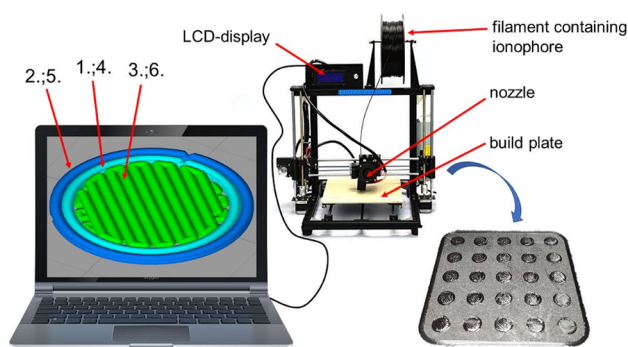
Fig. 5 The applied membrane design for 3D printing, the printer, and the fabricated membranes

by the reduced viscosity of the plasticized melted polymer fibers compared to pure PLA. (Although filaments with a diameter of 1.75 mm are most commonly used for 3D printers, the smaller fiber diameter is not a problem, because the fiber feed of the printer can be adjusted precisely.)

Different parts of the obtained ionophore-containing filament were used as raw material for 3D printing. There was no difference in the operating properties of the additively manufactured membranes made from the parts of the filament, which indicates that a filament of a sufficiently homogeneous composition was produced. Two-layer membranes of 200 μm thickness with a diameter of 8.0 mm were designed, which were compatible with the electrode body used in the electrochemical cell. Due to mechanical strength requirements, the lower limit of the allowable membrane thickness was 150 μm, while above 300 μm, a significantly increased response time of the membranes was observed, because of their reduced permeability. The membrane design and the printer unit are shown in Fig. 5.

The first step in printing was the construction of the inner perimeter as a border of the membrane (1 in Fig. 5), followed by the outer contour (2 in Fig. 5). After that the inner area of the membrane was filled with a parallel fiber direction (3 in Fig. 5). The primer layer must adhere properly to the build plate, thus a relatively high printing temperature of 175 °C was applied in the cases of polymers containing 20 wt% plasticizer. The next step was to continue creating the outer membrane contours by building a second membrane layer (4th and 5th steps in Fig. 5). Thereafter, the filling of the inner area was repeated, similarly to the first layer, with a layer thickness of 100 μm, but it was rotated by 90° in-plane (6 in Fig. 5). To form the second layer, a lower printing temperature of 170 °C was proved to be ideal in the cases of filaments containing 20 wt% plasticizer. The temperature of the build plate was optimally set to 55 °C, which provided proper solidification rate and adhesion of the membranes during the manufacturing. In terms of print speed (the moving speed of the nozzle), the highest value was 20 mm s^{-1}, which did not reduce the quality of the membranes. The printer was able to produce three membranes per minute at this speed; however, this performance strongly depends on the device. For filaments containing only 10 wt% plasticizer, higher temperatures had to be applied during printing, such as 200 °C for the first layer and 185 °C for the second one. The other device settings were the same as noted earlier.

A comparison of the microscopic images of the membranes (see Fig. 6) shows that membranes manufactured using PEG-1500 were the most regular, followed by the M-PEG-containing membranes and finally the PEG-400-containing ones, and among them the latter composition made processing difficult due to unfavorable rheological properties, thereby resulting in more irregular membranes.

Fortunately, these differences were not manifested in the electrochemical experiments. After optimization, 50–50 membranes from each investigated composition were prepared. Calculated from these statistical samples, the membrane thicknesses were within 200 ± 20 μm. These
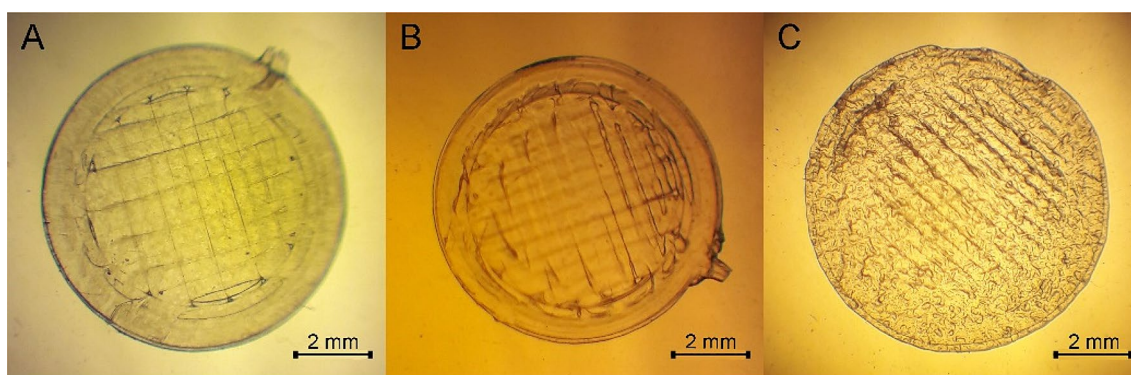
Fig. 6 3D-printed membranes containing various plasticizers in an amount of 20 wt% (**A** PEG-1500, **B** M-PEG, **C** PEG-400) and their diverse appearances influenced by different rheological properties in the manufacturing process

deviations did not affect the electrochemical performance of the membranes. The actual cross-sections between the gridlines on the rough surface can be much thinner as can be seen on SEM records in Fig. 7.

This property is due to the vertical manufacturing technology, which also produces an increased specific surface area compared to the conventional bulk membranes.

In summary, from the ionophore-containing plasticized PLA filaments produced by extrusion, a wasteless and environmentally friendly experimental series production of electrochemical membranes was realized in a cost-effective and time-saving manner using a commercially available and basic 3D printing device. After a thorough optimization of

the whole manufacturing process, production starting from the earlier mentioned batch (400 g plasticized PLA + 1.2 g ionophore) resulted in about 170-m filament line, which would be suitable for producing about 34,000 membranes. The production of the novel cation-selective membranes can be performed by a fully automated process. The ionophore is the only cost determinant among the components, as the total cost for production is at most 10 USD/10,000 membranes without counting the price of the ionophore. The membranes and the filament should be stored under airtight conditions until use. The membranes have to be soaked in distilled water for 5 min before use to ensure adequate wetting.

Fig. 7 Cross-sections of 3D-printed electrochemical membranes containing various plasticizers in an amount of 20 wt% (**A** PEG-1500, **B** M-PEG, **C** PEG-400) recorded by SEM
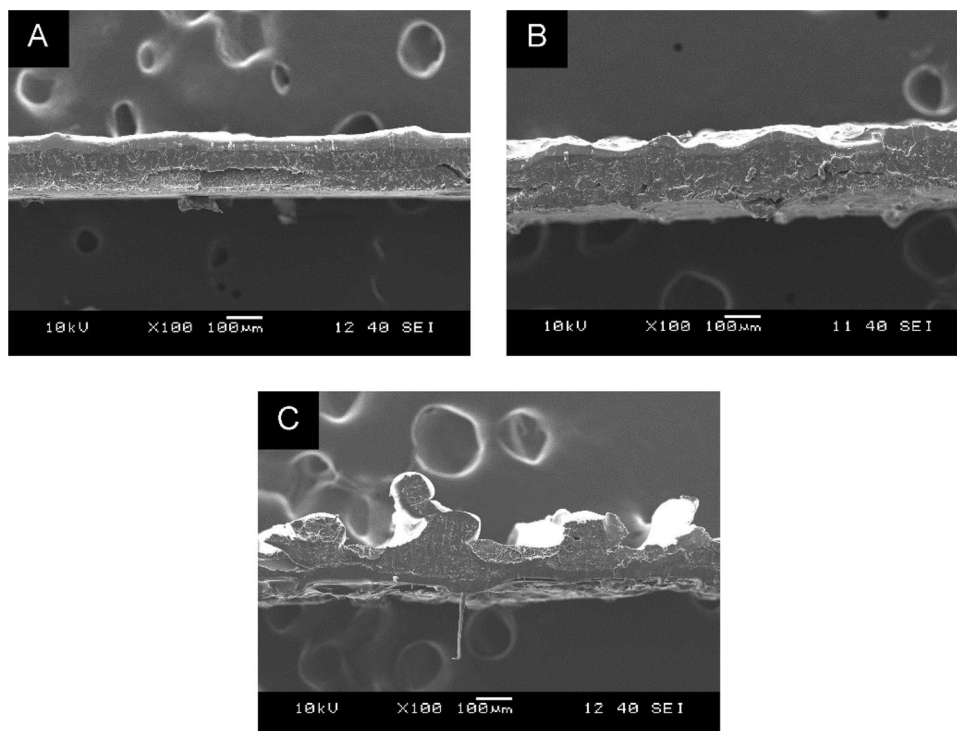
3.2 Proof-of-concept study on determination of Hg^{2+} in water

In order to verify the applicability of the new membrane fabrication technology and to demonstrate the efficiency of the novel membrane composition, 3D-printed membranes were incorporated into the same electrochemical cell, which had previously been successfully used for selective potentiometric detection of Pb^{2+} in water even under competitive conditions [37]. The ionophore used in the membrane was the same as in the case of the previously reported dioctyl sebacate (DOS)-plasticized, PVC-based traditional membranes containing potassium tetrakis(4-chlorophenyl)borate lipophilic ionic additive. Thus, potentiometric characterization of the novel electrode membranes was carried out and their characteristics were compared with those of the conventional ones.

First the electrodes containing differently plasticized 3D-printed membranes were calibrated with Pb^{2+} acetate aqueous solutions of different concentrations and then studies on selectivity were carried out. Surprisingly, the novel electrodes showed a preference for Hg^{2+} over Pb^{2+}, despite the ionophore previously found to be Pb^{2+} selective both in solution phase and inside PVC-based membranes. However, Hg^{2+} was the only ion, which caused interference in the case of the previously reported conventional Pb^{2+}-selective electrode. Presumably, the different polarities of the medium

and the reduced flexibility due to immobilization caused a change in the conformation of the ionophore, which altered its preference in molecular recognition. Based on this finding, Hg^{2+} was indicated as the primary ion and the calibration of the electrodes containing the novel membranes was consequently carried out with aqueous Hg^{2+} solutions, as shown in Fig. 8.

To the linear range of the calibration curve, a linear regression line (solid red line in Fig. 8) was fitted. The coefficient of determination (R^2) was higher than 0.99 in all cases. The ordinate value of the intersection of the regression line and the constant potential (horizontal dashed red line in Fig. 8) appoints the LOD. The results of electrochemical characterization are summarized in Table 2.

All the electrochemical properties of the novel membranes with 10 wt% plasticizer content were practically identical to those of the more plasticized version with the same plasticizer, the only difference was their significantly longer response time (about 5 min), and thus their use is not recommended due to this drawback. All of the electrodes gave a near-*Nernstian* response to the preferred ions with a linear working range in concentrations from 10^{-4} to 10^{-2} mol L^{-1} for conventional electrode membranes and from 10^{-6} to 10^{-2} mol L^{-1} for the novel ones. More than an order of magnitude decrease was also obtained in LOD due to the altered matrix material and manufacturing technology. The deviation was below ± 0.5 mV and the reproducibility

Fig. 8 Calibration curve of the conventional membrane electrode with Pb^{2+} (**A**) and the calibration curves of the novel ones (membranes containing **B** 20% PEG-400, **C** 20% PEG-1500, **D** 20% M-PEG) with aqueous Hg^{2+} solutions (deviations were within ± 0.5 mV in each case)
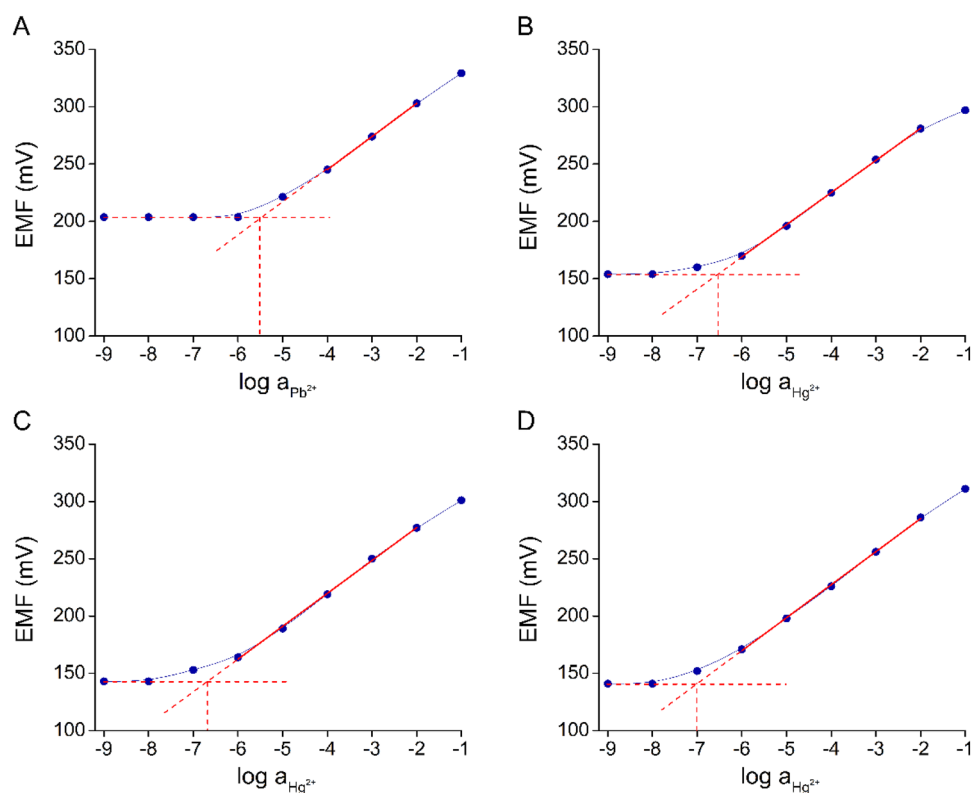
Table 2 Potentiometric characteristics of the investigated electrodes containing different ion-selective membranes

Membranes	Linear working range (mol L^{-1})	Slope[a] (mV/decade)	LOD (mol L^{-1})	Response time (s)
A[b]	10^{-4}–10^{-2}	28.9	4×10^{-6}	30
B[c]	10^{-6}–10^{-2}	28.0	4×10^{-7}	40
C[d]	10^{-6}–10^{-2}	28.7	3×10^{-7}	60
D[e]	10^{-6}–10^{-2}	28.8	1×10^{-7}	60

[a]The slope of the linear trendline fitted on the linear range of the potentiometric calibration curve

[b]The conventional-type PVC-based membrane containing 66 wt% DOS as plasticizer

[c]Novel-type 3D-printed PLA-based membrane containing 20 wt% PEG-400 as plasticizer

[d]Novel-type 3D-printed PLA-based membrane containing 20 wt% PEG-1500 as plasticizer

[e]Novel-type 3D-printed PLA-based membrane containing 20 wt% M-PEG as plasticizer

Table 3 Comparison of estimated potentiometric selectivity of the novel electrode membranes and their previously reported analogue as a reference

Ions	$\log K_{ij}^{\text{pot a}}$			
	A[b]	B[c]	C[d]	D[e]
Li$^+$	− 5.1	− 5.0	− 5.2	− 5.5
Na$^+$	− 5.0	− 4.9	− 5.0	− 5.3
Mg^{2+}	− 2.9	− 5.8	− 5.9	− 5.4
Zn^{2+}	− 2.9	− 5.9	− 5.7	− 5.1
K$^+$	− 4.4	− 4.6	− 4.8	− 3.3
Co^{2+}	− 2.9	− 4.8	− 5.0	− 4.9
Ca^{2+}	− 2.6	− 4.4	− 4.6	− 4.4
Cu^{2+}	− 2.5	− 5.1	− 5.3	− 4.5
Ag$^+$	− 4.0	− 2.6	− 3.1	− 2.9
Cd^{2+}	− 2.8	− 5.2	− 5.4	− 3.9
Hg^{2+}	− 0.8	0.0	0.0	0.0
Pb^{2+}	0.0	− 0.4	− 0.7	− 0.6

[a]In $\log K_{ij}^{\text{pot}}$ subscript i refers to the preferred ion, while subscript j refers to competing ions

[b]The conventional-type PVC-based membrane containing 66 wt% DOS as plasticizer

[c]Novel-type 3D-printed PLA-based membrane containing 20 wt% PEG-400 as plasticizer

[d]Novel-type 3D-printed PLA-based membrane containing 20 wt% PEG-1500 as plasticizer

[e]Novel-type 3D-printed PLA-based membrane containing 20 wt% M-PEG as plasticizer

was below ± 2.0 mV in each case. PLA-based membranes showed longer response times, but this is not significant in terms of the analytical performance.

The selectivity of the electrodes for various metal ions was assessed by recording the EMF response in the separate solutions of the preferred and interfering ions. Potentiometric selectivity was estimated using differences in the observed EMF values and the determined slope of the calibration curve. The potentiometric selectivity coefficients ($\log K_{ij}^{\text{pot}}$) reflect the ratio of the stability constants of the ionophore toward the preferred ion over various competing ions. It is important to note that without the possibility for exactly adjusting the amount of ion exchanger inside the membrane, the determined $\log K_{ij}^{\text{pot}}$ values could only give a rough estimate for the thermodynamic constants revealing the real interferences. Detailed discussion can be found in Sect. 3.3.

The potential response of the electrode was measured using 10^{-3} mol L^{-1} solutions of metal ions. The potentiometric selectivity coefficients for different interfering ions were standardized on Pb^{2+} in the case of the previously reported conventional electrode and on Hg^{2+} in the cases of the novel ones based on the observed highest preferences. The results are shown in Table 3.

It can be seen from the data that the novel membranes show advanced electrochemical properties and also an improved selectivity toward the majority of the investigated secondary ions compared to their conventional analogues. (In most of the cases, orders of magnitude improvements were obtained in estimated potentiometric selectivity constants.) The novel membranes showed the highest selectivity

toward Hg^{2+}. Unsurprisingly, Pb^{2+} was the only one among the investigated competing ions, which significantly interfered with Hg^{2+} determination. Although plasticizer PEG-1500 generally led to the best selectivity, LOD using M-PEG plasticizer proved to be the lowest. There was no significant difference in other operating parameters of membranes containing PLA matrix.

In contrast, studies on regenerability showed notable differences depending on the plasticizer. Since the water solubility of plasticizers PEG-400, PEG-1500, and M-PEG decreases in this order, this feature is also reflected in the regenerability. Although the same membrane was not used for potentiometric characterization (calibration, selectivity, etc.) to avoid disturbing effects, series of measurements involving Hg^{2+}-determination were carried out in 30 individual 10^{-4} mol L^{-1} aqueous samples to gain information on regenerability. No change was observed in working parameters during these studies, even after applying the same membranes for up to 30 measurements. An almost identical electrode response could be observed as in the case of the first sample with a deviation of less than ± 1.0 mV in the cases of membranes with less water-soluble plasticizers. In the cases of membranes plasticized with PEG-400, a reduced stability of the potentiometric response was observed. When

these membranes were immersed for more than 10 min into the aqueous samples, the electrochemical signal remained constant for about 4–5 min; however, after that time a gradient increasing drift was observed in response indicating that leaching of the hydrophile plasticizer probably takes place. Therefore, these membranes are single-use ones. For the other membrane compositions, this phenomenon was not observed during the measurements.

First of all, the M-PEG-plasticized membrane is considered to be the most stable one for monitoring of water samples and is also the most suggested one for other practical applications. In the future, it may be worth incorporating even more hydrophobic plasticizers into the membranes, such as the distearate derivative of PEG. The membranes could be stored under airtight conditions at 5 °C over a period of three months without any significant change in the calibration parameters.

3.3 Limitations

In contrast to conventional ion-selective bulk electrode membranes, the addition of lipophilic ionic components to provide permselectivity of the membranes was unnecessary since the partial degradation of PLA resulted in a sufficient number of free carboxylates inside the matrix for providing the ion-exchange function, which is essential for operation. This phenomenon can naturally be exploited only in the case of cation-selective membranes. Although the negative resulting charge of PLA is well established [35], studies were extended to support this concept. Membranes containing previously extruded PLA and potassium tetrakis(4-chlorophenyl)borate (generally used lipophilic anion exchanger) as well as the conventionally manufactured ones (evaporation of volatile solvent from a dispersion of the membrane cocktail containing all the components) without ionic additives were also prepared. The potentiometric calibration curves for these membranes can be seen in Fig. 9.

Results show that the calibration curve for conventionally manufactured membranes containing lipophilic anion exchanger (curve b) in part A of Fig. 9 is almost the same as that for the new 3D-printed membranes without ionic additives (curve a) in part A of Fig. 9. On the other hand, in the case of conventionally manufactured membranes without any ionic additive (curve b) in part B of Fig. 9, no *Nernstian* response was observed. The slope of the calibration curve significantly decreased and the deviation of the measurements increased, which all support the concept that, unless providing the essential ion-exchange for permselectivity, ionophores are unable to perform their function. These observations show that the negative resulting charge of the untreated PLA is not sufficient to perform the ion-exchange function of the membranes. The powerful shear forces and the intensive heat treatment during the extrusion result in an increased number of broken ester bonds, which makes the membrane surface sufficiently charged.

Consistently, in acidic conditions (pH < 6.0, see curves (c) and (d) in part A of Fig. 9), the quality of the potentiometric response deteriorated similarly. The carboxylate groups of the membrane matrix are expected to be protonated causing a decreased resulting charge strength, which makes the cations unable to enter the membrane unless breaking the rule of electroneutrality. It is also important to note that PLA hydrolyzes in acidic conditions. In the cases of measurements at pH ≤ 4.0, irreversible signal change and degradation of the corresponding membranes were observed. Therefore, the membranes should only be used in neutral medium (pH 6.0–7.0). It allows the majority of environmental samples to be analyzed without buffering.

In the case of conventional potentiometric ion-selective membranes, the optimal amount of the ion exchanger can exactly be determined in order to achieve the best possible selectivity toward the primary ion. In contrast, this is not possible in the case of the proposed, new 3D-printed PLA membranes, as the ratio of carboxylates responsible for permselectivity cannot be precisely adjusted. We can only strive to induce a minimum sufficient membrane charge for practical operation and to approach the ideal *Nernstian* response and thermodynamic selectivity values. In addition

Fig. 9 The potentiometric calibration curves for conventionally manufactured membranes containing previously extruded PLA plasticized with 20 wt% M-PEG and two equivalents (regarding the ionophore) of lipophilic anion exchanger (**A**) or those containing untreated PLA plasticized with 20 wt% M-PEG without any ionic additives (**B**)
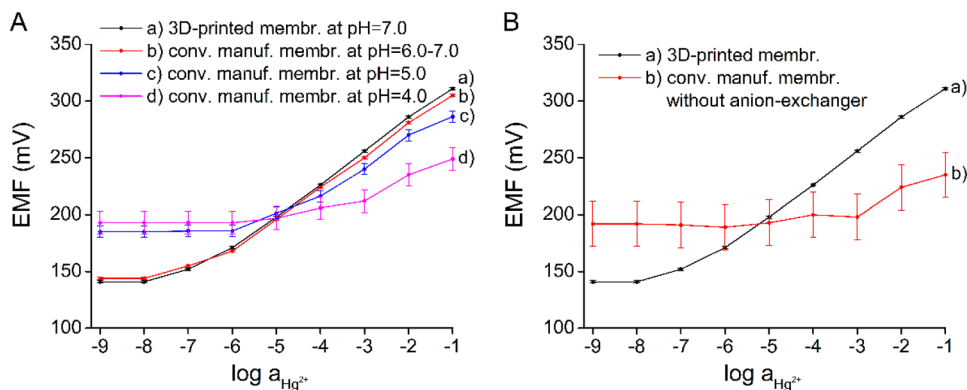
to the weak pH tolerance (pH = 6.0–7.0), the cation-targeted selectivity, and the relatively low chemical stability, it is clearly a drawback of the new type of membranes.

4 Conclusion

We have demonstrated a proof of concept for the series production and use of novel plasticized PLA-based ion-selective membranes for potentiometric sensing as greener alternatives to the conventional bulk electrode membranes. The proposed technology for production of cation-selective potentiometric membranes proved its effectiveness as a cheap, fast, precise, and automated manufacturing option with minimized waste. Extensive optimization of membrane composition and process parameters was carried out. The manufacturing technology resulted in the best quality in the case of PEG-1500-containing membranes. Depending on the ratio of the plasticizer, the value of 20 wt% proved to be the most favorable, of which the PEG-400-plasticized membranes were single-use ones, while others showed appropriate stability for practical applications. The new electrode, obtained by incorporating the novel 3D-printed membranes, was electrochemically characterized and compared to its conventional analogue using the generally applied DOS-plasticized PVC matrix and borate salts as lipophilic ionic additives. The novel membranes showed unexpected improvements in the majority of electrochemical properties, which involve a two-order magnitude wider linear working range, a more than one-order magnitude lower LOD, and an improved selectivity over Mg^{2+}, Zn^{2+}, Co^{2+}, Ca^{2+}, Cu^{2+}, and Cd^{2+}. Considering both electrochemical and stability parameters, 20 wt% M-PEG-containing two-layer membranes with 200 µm thickness proved to be the most advantageous ones. The main limitations of the novel membranes are the relatively low chemical stability and that the carboxylate content of the matrix (responsible for permselectivity) is not exactly adjustable, which only allows to approach the theoretical potentiometric response. The present results are believed to highly encourage the implementation of 3D printing technology in the preparation of cation-selective bulk membranes. Furthermore, these innovations could enable decentralized manufacturing and wide practical applications of cation-selective bulk membrane-based potentiometric sensors.

Declarations

References

1. Freiser H (2012) Ion-selective electrodes in analytical chemistry. Springer, New York
2. Crespo GA (2017) Recent advances in ion-selective membrane electrodes for in situ environmental water analysis. Electrochim Acta 245:1023–1034. https://doi.org/10.1016/j.electacta.2017.05.159
3. Myers RT, Ayers J (2019) A nitric oxide sensor fabricated through e-jet printing towards use in bioelectronics interfaces. J Appl Electrochem 49:229–239. https://doi.org/10.1007/s10800-018-1269-0
4. Gross B, Lockwood SY, Spence DM (2017) Recent advances in analytical chemistry by 3D printing. Anal Chem 89:57–70. https://doi.org/10.1021/acs.analchem.6b04344
5. Gordeev EG, Ananikov VP (2020) Widely accessible 3D printing technologies in chemistry, biochemistry and pharmaceutics: applications, materials and prospects. Russ Chem Rev 89:1507–1561. https://doi.org/10.1070/RCR4980
6. Yanar N, Kallem P, Son M, Park H, Kang S, Choi H (2020) A new era of water treatment technologies: 3D printing for membranes. J Ind Eng Chem 91:1–14. https://doi.org/10.1016/j.jiec.2020.07.043
7. Capel AJ, Rimington RP, Lewis MP, Christie SD (2018) 3D printing for chemical, pharmaceutical and biological applications. Nat Rev Chem 2:422–436. https://doi.org/10.1038/s41570-018-0058-y

8. Palenzuela CLM, Pumera M (2018) (Bio)Analytical chemistry enabled by 3D printing: sensors and biosensors. TrAC Trends Anal Chem 103:110–118. https://doi.org/10.1016/j.trac.2018.03.016

9. Lee JY, Tan WS, An J, Chua CK, Tang CY, Fane AG, Chong TH (2016) The potential to enhance membrane module design with 3D printing technology. J Membr Sci 499:480–490. https://doi.org/10.1016/j.memsci.2015.11.008

10. Rymansaib Z, Iravani P, Emslie E, Medvidović-Kosanović M, Sak-Bosnar M, Verdejo R, Marken F (2016) All-polystyrene 3D-printed electrochemical device with embedded carbon nanofiber-graphite-polystyrene composite conductor. Electroanalysis 28:1517–1523. https://doi.org/10.1002/elan.201600017

11. Loo AH, Chua CK, Pumera M (2017) DNA biosensing with 3D printing technology. Analyst 142:279–283. https://doi.org/10.1039/C6AN02038K

12. Lee KY, Ambrosi A, Pumera M (2017) 3D-printed metal electrodes for heavy metals detection by anodic stripping voltammetry. Electroanalysis 29:2444–2453. https://doi.org/10.1002/elan.201700388

13. Tan C, Nasir MZM, Ambrosi A, Pumera M (2017) 3D printed electrodes for detection of nitroaromatic explosives and nerve agents. Anal Chem 89:8995–9001. https://doi.org/10.1021/acs.analchem.7b01614

14. Krachunov S, Casson AJ (2016) 3D printed dry EEG electrodes. Sensors 16:1635–1652. https://doi.org/10.3390/s16101635

15. Muñoz J, Pumera M (2020) Accounts in 3D-printed electrochemical sensors: Towards monitoring of environmental pollutants. ChemElectroChem 7:3404–3413. https://doi.org/10.1002/celc.202000601

16. Cheng TS, Nasir MZM, Ambrosi A, Pumera M (2017) 3D-printed metal electrodes for electrochemical detection of phenols. Appl Mater Today 9:212–219. https://doi.org/10.1016/j.apmt.2017.07.005

17. Liyarita BR, Ambrosi A, Pumera M (2018) 3D-printed electrodes for sensing of biologically active molecules. Electroanalysis 30:1319–1326. https://doi.org/10.1002/elan.201700828

18. Cardoso RM, Mendonça DM, Silva WP, Silva MN, Nossol E, da Silva RA, Richter EM, Muñoz RA (2018) 3D printing for electroanalysis: from multiuse electrochemical cells to sensors. Anal Chim Acta 1033:49–57. https://doi.org/10.1016/j.aca.2018.06.021

19. Hamzah HH, Shafiee SA, Abdalla A, Patel BA (2018) 3D printable conductive materials for the fabrication of electrochemical sensors: a mini review. Electrochem Comm 96:27–31. https://doi.org/10.1016/j.elecom.2018.09.006

20. Manzanares Palenzuela CL, Novotný F, Krupička P, Sofer Z, Pumera M (2018) 3D-printed graphene/polylactic acid electrodes promise high sensitivity in electroanalysis. Anal Chem 90:5753–5757. https://doi.org/10.1021/acs.analchem.8b00083

21. Sfragano PS, Laschi S, Palchetti I (2020) Sustainable printed electrochemical platforms for greener analytics. Front Chem 8:644–650. https://doi.org/10.3389/fchem.2020.00644

22. Katseli V, Economou A, Kokkinos C (2019) Single-step fabrication of an integrated 3D-printed device for electrochemical sensing applications. Electrochem Comm 103:100–103. https://doi.org/10.1016/j.elecom.2019.05.008

23. João AF, Squissato AL, Richter EM, Muñoz RA (2020) Additive-manufactured sensors for biofuel analysis: copper determination in bioethanol using a 3D-printed carbon black/polylactic electrode. Anal Bioanal Chem 412:2755–2762. https://doi.org/10.1007/s00216-020-02513-y

24. Kalinke C, Neumsteir NV, de Oliveira Aparecido G, de Barros Ferraz TV, Dos Santos PL, Janegitz BC, Bonacin JA (2020) Comparison of activation processes for 3D printed PLA-graphene electrodes: electrochemical properties and application for sensing

25. Rocha DP, Squissato AL, da Silva SM, Richter EM, Munoz RA (2020) Improved electrochemical detection of metals in biological samples using 3D-printed electrode: chemical/electrochemical treatment exposes carbon-black conductive sites. Electrochim Acta 335:135688–135698. https://doi.org/10.1016/j.electacta.2020.135688

26. Wirth DM, Sheaff MJ, Waldman JV, Symcox MP, Whitehead HD, Sharp JD, Doerfler JR, Lamar AA, LeBlanc G (2019) Electrolysis activation of fused-filament-fabrication 3D-printed electrodes for electrochemical and spectroelectrochemical analysis. Anal Chem 91:5553–5557. https://doi.org/10.1021/acs.analchem.9b01331

27. Abdalla A, Patel BA (2020) 3D-printed electrochemical sensors: a new horizon for measurement of biomolecules. Curr Opin Electrochem 20:78–81. https://doi.org/10.1016/j.coelec.2020.04.009

28. Browne MP, Pumera M (2019) Impurities in graphene/PLA 3D-printing filaments dramatically influence the electrochemical properties of the devices. Chem Commun 55:8374–8377. https://doi.org/10.1039/C9CC03774H

29. Cardoso RM, Kalinke C, Rocha RG, dos Santos PL, Rocha DP, Oliveira PR, Janegitz BC, Bonacin JA, Richter EM, Munoz RA (2020) Additive-manufactured (3D-printed) electrochemical sensors: a critical review. Anal Chim Acta 1118:73–91. https://doi.org/10.1016/j.aca.2020.03.028

30. Bakker E, Bühlmann P, Pretsch E (1997) Carrier-based ion-selective electrodes and bulk optodes. 1. General characteristics. Chem Rev 97:3083–3132. https://doi.org/10.1021/cr940394a

31. Abdallah NA, Alahmadi YM, Bafail R, Omar MA (2021) Multi-walled carbon nanotubes/polyaniline covalently attached 18-crown-6-ether as a polymeric material for the potentiometric determination of delafloxacin. J Appl Electrochem. https://doi.org/10.1007/s10800-021-01636-z

32. Maksymiuk K, Stelmach E, Michalska A (2020) Unintended changes of ion-selective membranes composition−origin and effect on analytical performance. Membranes 10:266–279. https://doi.org/10.3390/membranes10100266

33. Qi X, Ren Y, Wang X (2017) New advances in the biodegradation of poly(lactic) acid. Int Biodeterior Biodegrad 117:215–223. https://doi.org/10.1016/j.ibiod.2017.01.010

34. Hamad K, Kaseem M, Ayyoob M, Joo J, Deri F (2018) Polylactic acid blends: the future of green, light and tough. Prog Polym Sci 85:83–127. https://doi.org/10.1016/j.progpolymsci.2018.07.001

35. Coolen AL, Lacroix C, Mercier-Gouy P, Delaune E, Monge C, Exposito JY, Verrier B (2019) Poly(lactic acid) nanoparticles and cell-penetrating peptide potentiate mRNA-based vaccine expression in dendritic cells triggering their activation. Biomaterials 195:23–37. https://doi.org/10.1016/j.biomaterials.2018.12.019

36. Riddick JA, Bunger WB, Sakano TK (1986) Organic solvents: physical properties and methods of purification (in the series: Techniques of chemistry). Wiley-Interscience, New York

37. Golcs Á, Horváth V, Huszthy P, Tóth T (2018) Fast potentiometric analysis of lead in aqueous medium under competitive conditions using an acridono-crown ether neutral ionophore. Sensors 18:1407–1420. https://doi.org/10.3390/s18051407

38. Bakker E, Pretsch E, Bühlmann P (2000) Selectivity of potentiometric ion sensors. Anal Chem 72:1127–1133. https://doi.org/10.1021/ac991146n

39. Abd El-Rahman MK, Salem MY (2015) Ion selective electrode (in-line analyzer) versus UV-spectroscopy (at-line analyzer); which strategy offers more opportunities for real time monitoring of the degradation kinetics of pyridostigmine bromide. Sensors Actuators B 220:255–262. https://doi.org/10.1016/j.snb.2015.05.092

40. Martin O, Avérous L (2001) Poly(lactic acid): plasticization and properties of biodegradable multiphase systems. Polymer 42:6209–6219. https://doi.org/10.1016/S0032-3861(01)00086-6